Mater.Phys.Mech.1 (2000) 133-139

A DISCLINATION-BASED MODEL FOR ANISOTROPIC SUBSTRUCTURE DEVELOPMENT AND ITS IMPACT ON THE CRITICAL RESOLVED SHEAR STRESSES

M. Seefeldt and P. Van Houtte

Catholic University of Leuven, Department of Metallurgy and Materials Engineering,
de Croylaan 2 B-3001 Heverlee, Belgium

Received: June 25, 2000

Abstract. The anisotropic mechanical response of f.c.c. metals deformed up to large strains at low homologous temperatures is controlled by interfaces, namely by fragment and grain boundaries. The proposed model starts from initial grain orientations and the corresponding slip rates as predicted by a full constraints (FC) Taylor code. It describes the cell structure development on the microscopic scale and the fragment structure development on the mesoscopic scale in terms of evolution equations for dislocation densities in the twelve f.c.c. slip systems and for disclination densities in six fragment boundary families, respectively. The redundant dislocation densities (or: the cell walls) and the immobile disclination densities and strengths (or: the fragment boundary triple junctions) are connected to critical resolved shear stress (CRSS) contributions. Thus, substructure and texture evolution as well as the resulting macroscopic mechanical behaviour are coupled to each other. Results for several initial grain orientations are presented and compared to experimental observations.

1. INTRODUCTION

Grain subdivision or fragmentation gains more and more interest in materials science and technology since it turns out to be the essential substructural feature at large strain plastic deformation and thus in all technically relevant forming processes. Especially, severe plastic deformation (SPD) [1] results into extensive fragmentation. SPD is used to produce ultra-fine grained (UFG) materials which combine a very high strength with good formability. Therefore, the mechanical properties of UFG materials can be understood as fragment boundary controlled.

If this fragmentation process is based on nucleation and growth of dislocation rotation boundaries, the formation, spread-out and enlargement of misorientation across fragment boundaries which develop along existing cell walls can properly be described in terms of generation, propagation and immobilization of partial disclination dipoles [2,3]. A model for the substructure development under plastic deformation of f.c.c. materials up to large strains can then be formulated in terms of coupled rate equations for dislocation and disclination densities describing the cell and fragment structure developments, respectively.

Partial disclination dipoles – corresponding either to both-side terminating excess dislocation walls or to pairs of parallel terminating excess dislocation boundaries of opposite sign [3] – can be formed by incidental, non-compensated trapping of neighbouring mobile dislocations of the same sign (see Figs. 1a and 1b) [4] or stress-induced at grain boundary edges or triple junctions [5]. The partials of both types can propagate by capturing additional mobile dislocations of the "right" character and sign with the help of their long-range stress fields (see Figs. 1c and 1d) [3,6]. Propagating partial disclinations get stuck in the network of already existing fragment boundaries, thereby leaving an orientation mismatch behind (see Fig. 2), as could recently be confirmed by TEM microdiffraction measurements [7]. STM investigations revealed an enhanced volume energy content around the triple junctions [8].

Therefore, the triple junctions of fragment boundaries include immobile partial disclinations. The hard cell walls give rise to a shear resistance [9], the long-range stress fields around the non-compensated triple junctions to a tilt resistance, so that the redundant dislocation densities and the immobile disclination densities and strengths can be coupled to flow stress contributions.

Corresponding author: M. Seefeldt, e-mail: Marc.Seefeldt@mtm.kuleuven.ac.be

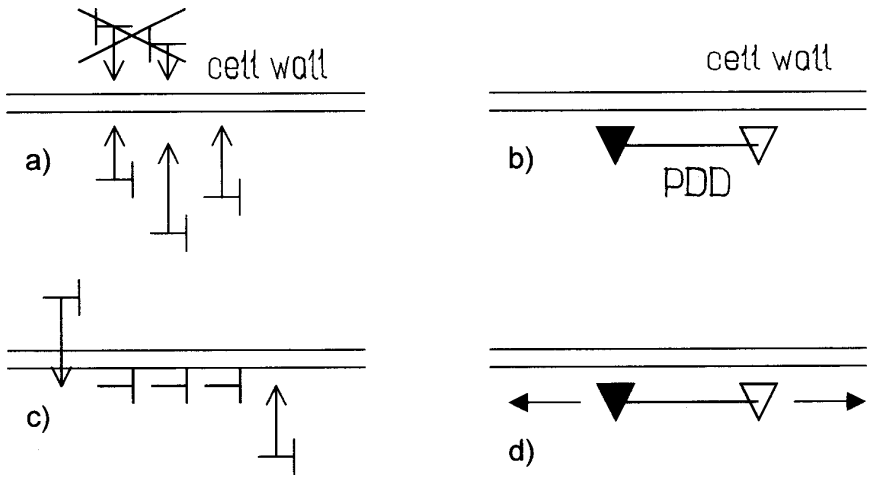

Fig. 1. Elementary processes: a) Incidental trapping of neighbouring mobile excess dislocations of the same sign and character at a cell wall. The crossed-out dislocations indicate that the trapped ones must not be balanced in order to form a nucleus of misorientation. b) The resulting excess dislocation group described as a partial disclination dipole (PDD, the filled and unfilled triangle denoting the positive and the negative partial, respectively). c) Expansion of the group by capturing additional mobile dislocations. d) Expansion of the PDD by propagation of its partials.

2. SUMMARY OF THE "ISOTROPIC MODEL" FOR MONOCRYSTALS

Based on this scenario, an "isotropic model" for the cell and fragment (or cell block) structure evolutions and their impact on the macroscopic mechanical behaviour has been developed for monocrystals under uniaxial deformation up to large strains [4,10]. The substructure has been schematized in terms of global average densities of mobile and redundant cell wall dislocations as well as of mobile and immobile partial disclinations. Evolution equations derived from the underlying elementary processes have been put up and allow to describe the cell and fragment size as well as the fragment boundary misorientation development in good agreement with experiment. Especially, a saturation of the cell structure, a hyperbolic decrease of the mean fragment size and an almost linear increase of the mean misorientation across fragment boundaries are reproduced. The redundant dislocation densities and the immobile disclination densities and strengths are connected to flow stress contributions. A flow curve recorded from a quasistatic room temperature compression test on a copper single crystal is well reproduced. Particularly, stage III behaviour can be attributed to dislocation (or cell wall), stage IV behaviour to disclination (or fragment boundary triple junction) hardening.

3. AN "ANISOTROPIC MODEL" FOR POLYCRYSTALS

From the scientific as well as from the technological point of view, it is desirable to extend this model to the plastic deformation of polycrystalline materials under complex loading conditions. For that purpose, anisotropy has to be taken into account on three interacting levels [11]: Following from the anisotropic slip geometry, the substructure, especially the fragment structure, turns out to be also strongly anisotropic. Furthermore, its development influences the texture evolution through misorientations and work-hardening. Therefore, the fragment structure is likely to contribute significantly to the macroscopic mechanical anisotropy.

In order to take the anisotropy of slip into account, the present model describes the substructure development in terms of separate evolution equations [12] for

- mobile dislocation densities in the twelve f.c.c. slip systems, incidentally stored (redundant) cell wall dislocation densities in six cell wall families,
- propagating partial disclination densities in the six cell wall and fragment boundary families, and
- immobile partial disclination densities in the fragment boundary families.

To calculate misorientations, in addition, the

- geometrically necessary (non-redundant) dislocation densities in the six fragment boundary families

have to be calculated. The six cell wall families are constructed according to the following scheme: Each cell wall is assumed to be formed as a result of interactions between mobile and forest dislocations in two different slip planes corresponding to two intersecting surfaces of Thompson's tetrahedron. Thus, the six cell wall families correspond to the six edges of the tetrahedron. The dislocations in each of the three slip systems belonging to one of the two slip planes can for-

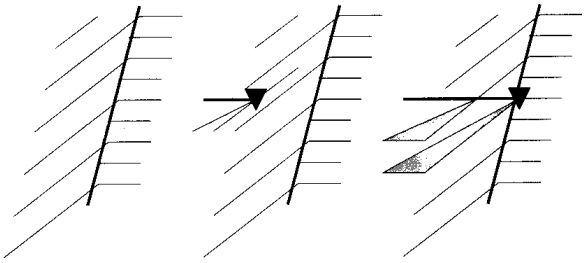

Fig. 2. Elementary processes: Generation of a non-compensated fragment boundary triple junction. The partial disclination propagating at the top of the "new" fragment boundary rotates the two shores of the boundary with respect to each other (here, for simplicity, only indicated below the boundary). When it gets stuck in the "old" fragment boundary, an orientation mismatch is left behind (shaded, cf. the term "wedge" disclination). If this mismatch is compensated by elastic distortion, the triple junction includes a partial disclination.

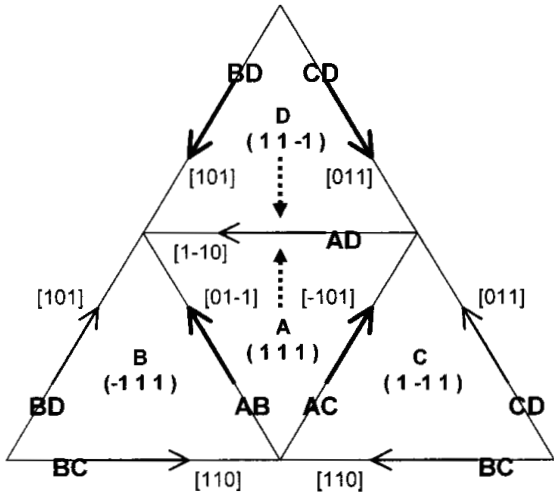

Fig. 3. Fold-up Thompson tetrahedron with slip planes A-D and cell wall families AB-CD. As an example, the bold arrows indicate the four slip systems which participate in the formation of the cell wall family AD, if only edge dislocations are considered. In the case of symmetric activation, combined mobile edge dislocations would glide in the directions indicated by the dotted arrows, undergo parallel interaction and form cell walls parallel to the edge AD. Thus, the six edges of the tetrahedron correspond to the six cell wall families.

mally be decomposed into segments undergoing either parallel or junction interaction with the corresponding segments in the other slip plane. Since most of the junction interactions result into non-correlated Orowan cutting processes, it is assumed that the wall is formed by parallel interaction and, later on, filled up and consolidated by junction interaction. Consequently, the cell wall normal should be perpendicular to the intersection line of the two slip planes and inclined according to the respective activation of the slip systems in the two slip planes.

As an example, Fig. 3 illustrates this scheme for the case of pure edge dislocations under symmetric activation of eight slip systems. The four slip systems with Burgers vectors non-parallel to the intersection line of their slip planes can be collected into two combined slip systems contributing to parallel interaction and controlling the cell wall orientation.

In order to put up the evolution equations, the following elementary processes are taken into account: Multiplicative generation of mobile dislocations, immobilization of mobile dislocations at cell walls, annihilation of mobile with cell wall dislocations, generation of partial disclination dipoles by incidental non-balanced trapping of neighbouring excess dislocation, partial disclination propagation by capture of additional mobile dislocations, and immobilization of propagating partial disclinations in the network of immobile partial disclinations.

Mobile dislocations can be immobilized at each cell wall which is not parallel to the dislocations' slip direction. The trapping probability depends on whether the wall is formed from dislocations parallel or non-parallel to the approaching one. The immobilization rate for a slip system (i) thus scales with the sum of the inverse cell wall spacings $d_c^{(w)}$ in the wall families (w) weighted with factors $I_p=2\,P_p\,f_{geom}/b$ or $I_j=2\,P_p\,f_{geom}/b$ (essentially including the trapping probabilities P_p and P_j for parallel or junction interaction, respectively) and the slip rate $\dot{\gamma}^{(i)}$. On the other hand, mobile dislocations can annihilate with cell wall dislocations from the same slip system, but of opposite sign, by spontaneous disintegration. The recovery rate thus scales with the cell wall dislocation density $\rho_c^{(i)}$ in the slip system (i) weighted with a factor $R=2ya/b$ (essentially including the annihilation length y_a). Finally, one arrives at an evolution equation for the cell wall dislocation density $\rho_c^{(i)}$ in the slip system (i) of

$$\frac{d\rho_c^{(i)}}{dt}=\left(\left(\sum_{w_p(i)}\frac{I_p}{d_c^{(w_p(i))}}+\sum_{w_j(i)}\frac{I_j}{d_c^{(w_j(i))}}\right)-R\,\rho_c^{(i)}\right)\dot{\gamma}^{(i)}, \quad (1)$$

where the indices $w_p^{(i)}$ and $w_j^{(i)}$ run over all cell wall families (w) which act as parallel or junction interaction obstacles, respectively, to the mobile dislocations in slip system (i). The cell wall spacings $d_c^{(w)}$ are assumed to follow a Holt-type scaling law with an average Holt constant K,

$$d_c^{(w)}=\frac{K}{\sqrt{\sum_{i_p(w)}f_p^{(i\to w)}\rho_c^{(i_p(w))}+\sum_{i_j(w)}f_j^{(i\to w)}\rho_c^{(i_j(w))}}}, \quad (2)$$

where $f_p^{(i\to w)}$ and $f_j^{(i\to w)}$ denote the fractions of the cell wall dislocation densities $\rho_c^{(i)}$ from slip system (i) which are stored in cell walls belonging to the family (w). The indices $i_p^{(w)}$ and $i_j^{(w)}$ run over all slip systems (i) forming or filling up the wall family (w). Note that inserting Eq. 2 into Eq. 1 and applying Orowan's law to transform Eq. 1 from the evolution parameter time to the evolution parameter strain gives a slip system-resolved variant of Kocks' storage and recovery evolution equation [13].

Partial disclination dipoles are generated by incidental and non-balanced trapping of neighbouring mobile dislocations of the same character and sign either at cell walls or fragment boundaries (see Figs. 1a and 1b). However, both-side terminating boundary segments consisting of parallel straight excess dislocations can only be formed by parallel interaction because junction interaction would rather leave Orowan loops and other dislocation debris with non-correlated and thus non-accumulating signs behind. Consequently, only those slip systems can contribute to partial disclination generation at a certain cell wall whose mobile dislocations undergo parallel interaction with the cell wall dislocations which have originally formed the cell wall (by parallel interaction). The partial disclination dipole generation rate in one cell wall family has a structure similar to the one of the dislocation immobilization rate discussed above. It is scaled with the inverse of the cell wall and the cell block boundary spacings weighted with the factors K_c or K_{cb}, respectively. However, these factors do not only include the trapping probability, but the product of the probability of a dislocation being trapped on one side of the wall or boundary and the probability of the dislocation approaching the wall or boundary from the other side at the same time not being trapped, raised to the power N to take the required collective behaviour of N neighbouring dislocations into account, $K_c=2(P_p(1\text{-}P_p))^N f_{geom}/b$ and $K_{cb}=2(P_{cb}(1\text{-}P_{cb}))^N f_{geom}/b$.

Furthermore, the mobile dislocations in those slip systems allow the partial disclinations to propagate: They are captured by the partial disclinations' long-range stress fields [6]. Thus, additional excess dislocations are attached to the boundary segments, the boundary edges are moved, the corresponding partial disclinations propagate, the partial disclination dipole expands. Consequently, the partial disclination velocity is controlled by the sum of the slip rates in those slip systems whose mobile dislocations contribute to partial disclination dipole generation. Neglecting the peculiarities of the accelerated motion of mobile dislocations being captured, it is assumed, that all dislocations of the "right" character and sign passing a partial disclination within a capturing length y_c are attached to the partial disclinations' backward fragment boundary. Comparing the stress $\tau_{PD}+\tau_{ext}$ due to the partial disclination and the external load to the resistance τ^* due to a statistical distribution of mobile dislocations gives an estimate capturing length of about $y_c\approx 10a$ where a is the half disclination dipole width [14]. The partial disclination velocity in the cell wall and fragment boundary family (w) then is

$$V^{(w)}=\frac{5a}{2\omega}\sum_{i_p(w)}\dot{\gamma}^{(i_p(w))}. \tag{3}$$

Finally, the propagating partial disclinations get stuck in the network of existing fragment boundaries. Their immobilization rate has a similar structure as the one for the dislocations discussed above: It scales with the inverse spacing $d_{cb}^{(w)}$ between the fragment boundaries of its own family and with the propagating partial disclination current $V^{(w)}\theta_m^{(w)}$ resulting into the evolution equation

$$\frac{d\theta_m^{(w)}}{dt}=\left(\frac{K_c/N}{d_c^{(w)}}+\frac{K_{cb}/N}{d_{cb}^{(w)}}-\frac{J}{d_{cb}^{(w)}}\theta_m^{(w)}\right)\sum_{i_p(w)}\dot{\gamma}^{(i_p(w))}. \tag{4}$$

The corresponding evolution equation for the immobile partial disclination densities in the fragment boundary triple junctions reads

$$\frac{d\theta_i^{(w)}}{dt}=\frac{J}{d_{cb}^{(w)}}\theta_m^{(w)}\sum_{i_p(w)}\dot{\gamma}^{(i_p(w))}. \tag{5}$$

For a simple parallelepipedal mosaic geometry with elongated fragments and small boundary thicknesses, the boundary spacings follow the scaling law

$$d_{cb}^{(w)}=\frac{1}{\sqrt{2\theta_i^{(w)}}}. \tag{6}$$

In order to calculate the average misorientation across the fragment boundaries of a family (w), one has to distribute those excess dislocations which have either formed or been captured by partial disclination dipoles propagating along walls or boundaries of (w) on the available total boundary length in this family:

$$\phi_{cb}^{(w)}=\frac{bp_{exc}^{(w)}}{2d_{cb}^{(w)}}. \tag{7}$$

The corresponding evolution equation reads

$$\frac{d\rho_{exc}^{(w)}}{dt}=\left(\frac{K_c}{d_c^{(w)}}+\frac{K_{cb}}{d_{cb}^{(w)}}-E\theta_m^{(w)}\right)\sum_{i_p(w)}\dot{\gamma}^{(i_p(w))}, \tag{8}$$

where the reaction coefficient $E=y_c/b$ reflects the capturing process in a similar way like $R=2y_a/b$ the annihilation process. Using the slip rates generated by a full constraints Taylor algorithm (see e.g. [15]), the evolution Eqs. 1, 4, 5 and 8 can be integrated numerically. The relations 2, 6 and 7 then characterize the substructure development.

Finally, the immobile defect densities can be connected to critical resolved shear stress contributions in the twelve slip systems. For the dislocation or cell structure contribution, again a parallel and a junction interaction term have to be distinguished. Following Franciosi's proposal [16], the two terms are superimposed in a harmonic instead of in a linear way,

$$\Delta\tau_{\rho}^{crit(i)} = Gb\sqrt{\sum_{w_p(i)}\frac{A_p}{d_c^{(w_p(i))^2}} + \sum_{w_j(i)}\frac{A_j}{d_c^{(w_j(i))^2}}}. \qquad (9)$$

Since $\Delta\tau_{\rho} = \xi\alpha Gb\sqrt{\rho_w} = \xi\alpha Gb\sqrt{\rho_c/\xi} = \sqrt{\xi}\alpha G \times bK/d_c$ (ξ – cell wall volume fraction, K – Holt-type constant) holds for the shear resistance of compounds with dislocation-free cell interiors, one can assess $A_p=0.25\xi\alpha^2K^2$ and $A_p=4\xi\alpha^2K^2$, where the number factors ensure that junction interaction is about four times stronger in aluminium than parallel interaction (see [16]). Correspondingly, the formula $\Delta\tau_{\theta}=\beta G\omega(\varepsilon)\approx\beta G\phi(\varepsilon)$ for the shear resistance due to a regular arrangement of partial disclinations [3] can be adapted to give

$$\Delta\tau_{\theta}^{crit(i)} = G\sqrt{B_p\sum_{w_p(i)}\omega_{cb}^{(w_p(i))}} \approx G\sqrt{B_p\sum_{w_p(i)}\phi_{cb}^{(w_p(i))}} \qquad (10)$$

with $B_p=1/4\beta^2$.

4. RESULTS AND DISCUSSION

Substructure Evolution. For aluminium single crystals of several standard orientations, the model predictions on the substructure development can be compared to TEM results [17-19].

For the brass orientation {110}<112> under cold rolling up to 45 % thickness reduction (ε=0.5 von Mises equivalent strain), Godfrey et al. [17] found one well-pronounced set of short cell walls and long cell block boundaries parallel to (-1 1 1) slip plane traces, and a less pronounced set of walls and boundaries close to (-1 -1 1) slip plane traces. Cell walls in the first set carried an average misorientation of $\bar{\phi}_c$=1.4, cell block boundaries in the first set of $\bar{\phi}_{cb}$=1.6° with a maximum of ϕ_{cb}^{max}=5.4°, walls and boundaries in the second set of about $\bar{\phi}_c$=1.3°. After 78 % thickness reduction, (ε=1.5 von Mises equivalent strain), the average misorientation across cell block boundaries in the first set increased up to $\bar{\phi}_{cb}$=2.2°, while the others remained essentially unchanged.

The present model predicts two well-pronounced sets of cell walls and cell block boundaries as well as two well-pronounced sets only of cell walls. Under the assumption that the walls and boundaries are oriented according to the relative activation of the slip systems in the two slip planes involved in their formation, the first mixed set lies close to (-1 1 1) slip planes, while the second one is parallel to the rolling plane. The two cell wall sets lye close to the (-1 -1 1) slip planes. At ε=0.5, the first cell wall and cell block boundary set shows average spacings of $\bar{d}_c$=1.99 μm and $\bar{d}_{cb}$=2.86 μm and an average misorientation of $\bar{\phi}_{cb}$=2.68°, while the second one is characterized by $\bar{d}_c$=1.94 μm, $\bar{d}_{cb}$=2.52 μm and $\bar{\phi}_{cb}$=2.74°. The two cell wall sets show average spacings of $\bar{d}_c$=1.99 μm and $\bar{d}_c$=1.83 μm.

For the copper orientation {112}<111> under cold rolling up to 45 % thickness reduction, Godfrey et al. [18] found one well-pronounced set of cell walls and cell block boundaries close to the codirectional (1 -1 1)[011] and (-1 -1 1)[011] slip plane traces, one less-pronounced set with typical pairs of cell block boundaries close to the coplanar (-1 1 1)[101] and (-1 1 1)[-1 -1 0] slip plane traces, and some narrow bands forming an angle of about 35° with the rolling direction crossing between the coplanar bands. At 45 % thickness reduction, the codirectional set dominated with misorientations of about $\bar{\phi}_c$=2.0° across cell walls and of about $\bar{\phi}_{cb}$=3.4° across cell block boundaries. After 78 % thickness reduction, the codirectional set was essentially unchanged, while the coplanar set displayed misorientations of about $\bar{\phi}_{cb}$=5.3° across cell block boundaries.

The model predicts two well-pronounced sets of cell walls and cell block boundaries close to the (-1 1 1) and (1 -1 1) slip plane traces corresponding to the two codirectional active slip systems and a significantly less pronounced set parallel to the (-1 1 1) slip plane corresponding to the two coplanar active slip systems. At ε=0.5, the two codirectional sets show average spacings of $\bar{d}_c$=1.13 μm and $\bar{d}_{cb}$=0.55 μm or $\bar{d}_c$=0.97 μm and $\bar{d}_{cb}$=2.48 μm, respectively, and average misorientations of $\bar{\phi}_{cb}$=2.74° or $\bar{\phi}_{cb}$=2.75°, respectively. On the other hand, the coplanar set exhibits spacings of $\bar{d}_c$=1.17 μm and $\bar{d}_{cb}$=4.26 μm and a misorientation of $\bar{\phi}_{cb}$=2.69°.

In order to demonstrate the dependence of the cell and fragment structure evolutions on the initial monocrystal or grain orientation, Fig. 4 displays the simulated cell wall and cell block boundary spacing developments

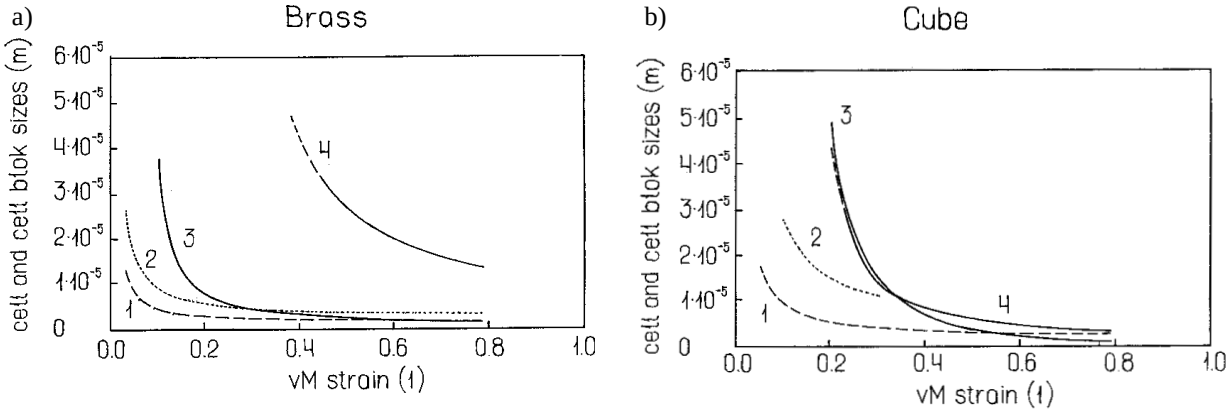

Fig. 4. Development of the mean cell wall (cw) and mean cell block boundary (cbb) spacings for aluminium monocrystals of cube and brass orientation. Only the curves for the cw and cbb families with the minimum and maximum spacings are displayed. (a): 1 – cw spacing CD; 2 – cw spacing AD, BD; 3 – cbb spacing AB; 4 – cbb spacing BD. (b): 1 – cw spacing AB, AD, BC, CD; 2 – cw spacing BD; 3 – cbb spacing AD, CD; 4 – cbb spacing BC.

with the von Mises equivalent strain for the brass and the cube orientations.

Critical resolved shear stresses. The critical resolved shear stress contributions due to the redundant dislocations in the cell walls and due to the immobile partial disclinations in the fragment boundary triple junctions according to Eqs. 9 and 10 are presented for the brass orientation in Fig. 5. While the cell structure contribution is nearly the same for all active slip systems, the fragment structure contribution differs considerably from slip system to slip system. Consequently, a substructure contribution to anisotropic hardening can be ascribed to the fragment structure.

The results listed above have been obtained without taking work-hardening into account in the full constraints Taylor code. A forthcoming paper [20] will present simulations based on a full coupling between substructure and texture evolution, a systematic study of the dependence of the substructure development on the initial grain orientation and model predictions on the anisotropic macroscopic mechanical behaviour.

5. CONCLUSIONS

A model for the development of the cell and fragment structures and the corresponding critical resolved shear stress contributions under plastic deformation up to large strains has been outlined. The substructure is represented by the mobile, redundant (cell walls) and excess (fragment boundaries) dislocations as well as by the mobile and immobile (fragment boundary triple junctions) partial disclination densities in the twelve f.c.c. slip systems or in six cell wall and fragment boundary families. Evolution equations based on physical elementary processes are put up. Using the slip rates generated by a full constraints Taylor algorithm, these equations can be integrated numerically to predict the developments of the cell wall and fragment boundary spacings, and of the misorientations across the fragment boundaries in the six families. The critical resolved shear stress contributions due to the cell walls (dislocations) and fragment boundary triple junctions (partial disclinations) are estimated.

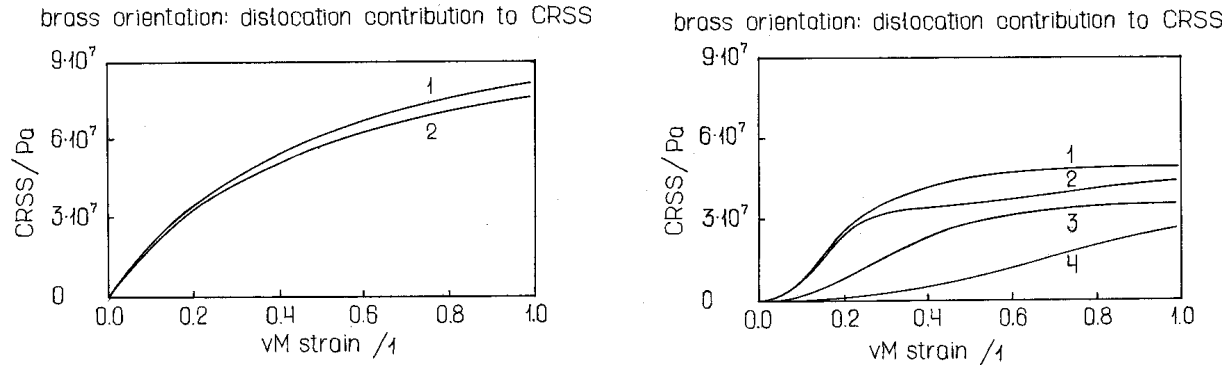

Fig. 5. Development of the critical resolved shear stress (crss) contributions due to dislocations (in the cell walls) and disclinations (in the fragment boundary triple junctions), respectively, for an aluminium monocrystal of brass orientation. Only the curves for the four active slip systems are displayed. (a): 1 – A3, 2 – B2; (b): 1 – A3, 2 – B2, 3 – D2, 4 – D3.

The model is capable of predicting the substructure evolution for aluminium single crystals of several standard orientations in reasonable agreement with the (rare) experimental data. A substructure contribution to anisotropic hardening can clearly be attributed to the fragment structure.

ACKNOWLEDGEMENTS

The authors thank L. Delannay and B. Peeters, Leuven, for helpful discussions. Financial support given by the European project BE-97-4135 is gratefully acknowledged.

REFERENCES

[1] *Investigations and Applications of Severe Plastic Deformation, Proceedings of the NATO Advanced Research Workshop, Moscow, Russia, 2-7 August 1999*, ed. by T.C. Lowe and R.Z. Valiev, NATO Science Series 3/80 (Kluwer, Dordrecht, 2000).

[2] V.V. Rybin, *Large Plastic Deformation and Fracture of Metals* (Metallurgiya, Moskva, 1986) (in Russian).

[3] A.E. Romanov and V.I. Vladimirov, *Disclinations in Crystalline Solids*, in: *Dislocations in Solids*, vol. **9**, ed. by F.R.N. Nabarro (North Holland, Amsterdam, 1992), p. 191.

[4] M. Seefeldt, V. Klemm and P. Klimanek, in *Investigations and Applications of Severe Plastic Deformation, Proceedings of the NATO Advanced Research Workshop, Moscow, Russia, 2-7 August 1999*, ed. by T.C. Lowe and R.Z. Valiev, NATO Science Series 3/80 (Kluwer, Dordrecht, 2000), p. 197.

[5] M. Gutkin, A.E. Romanov and P. Klimanek, *Local Lattice Rotations and Disclinations in Microstructures of Distorted Crystalline Materials*, Proceedings of the International Workshop, Rauschenbach, Germany, 10-14 April 2000, ed. by P. Klimanek.

[6] V.I. Vladimirov and A.E. Romanov // *Fiz. Tverd. Tela* **20** (1978) 3114.

[7] V. Klemm, P. Klimanek and M. Seefeldt // *Phys. Stat. Sol. (a)* **175** (1999) 569.

[8] M. Seefeldt // *Mater. Phys. Mech.* **1** (2000) 54.

[9] H. Mughrabi // *Acta metall.* **31** (1983) 1367.

[10] M. Seefeldt and P. Klimanek // *Modelling Simul. Mater. Sci. Eng.* **6** (1998) 349.

[11] B. Peeters, S.R. Kalidindi, P. Van Houtte and E. Aernoudt // *Acta mater.* **48** (2000) 2123.

[12] A.N. Orlov // *Fiz. Met. Metalloved.* **20** (1965) 12.

[13] U.F. Kocks // *Transactions of the ASME – Journal of Engineering Materials and Technology* **98** (1976) 76.

[14] M. Seefeldt, *Modellierung der Substrukturentwicklung bei Kaltumformung mit Hilfe von Disklinationen*, Ph.D. thesis, Freiberger Forschungsheft B 304 (TU Bergakademie Freiberg, Freiberg, 2000).

[15] E. Aernoudt, P. Van Houtte and T. Leffers, *Deformation and Textures of Metals at Large Strain, in: Materials Science and Technology*, ed. by R.W. Cahn, P. Haasen and E.J. Kramer, vol. 6, *Plastic Deformation and Fracture of Metals*, ed. by H. Mughrabi (VCH, Weinheim, 1993), p. 89.

[16] P. Franciosi // *Acta metall.* **33** (1985) 1601.

[17] A. Godfrey, D. Juul Jensen and N. Hansen // *Acta mater.* **46** (1998) 823.

[18] A. Godfrey, D. Juul Jensen and N. Hansen // *Acta mater.* **46** (1998) 835.

[19] Q. Liu and N. Hansen // *Proc. R. Soc. Lond. A* **454** (1998) 2555.

[20] M. Seefeldt, L. Delannay, B. Peeters, P. Van Houtte and E. Aernoudt, forthcoming.